# 4

# Vibration Responses of Atomic Force Microscope Cantilevers

Thin-Lin Horng
*Department of Mechanical Engineering, Kun-Shan University, Tainan Taiwan, R.O.C.*

## 1. Introduction

In this investigation, the solution of the vibration response of an atomic force microscope cantilever is obtained by using the Timoshenko beam theory and the modal superposition method. In dynamic mode atomic force microscopy (AFM), information about the sample surface is obtained by monitoring the vibration parameters (e.g., amplitude or phase) of an oscillating cantilever which interacts with the sample surface. The atomic force microscope (AFM) cantilever was developed for producing high-resolution images of surface structures of both conductive and insulating samples in both air and liquid environments (Takaharu et al., 2003 ; Kageshima et al., 2002 ; Kobayashi et al., 2002 ; Yaxin & Bharat, 2007). In addition, the AFM cantilever can be applied to nanolithography in micro/nano electromechanical systems (MEMS/NEMS) (Fang & Chang, 2003) and as a nanoindentation tester for evaluating mechanical properties (Miyahara, et al., 1999). Therefore, it is essential to preciously calculate the vibration response of AFM cantilever during the sampling process. In the last few years, there has been growing interest in the dynamic responses of the AFM cantilever. Horng (Horng, 2009) employed the modal superposition method to analyze the vibration responses of AFM cantilevers in tapping mode (TM) operated in a liquid and in air. Lin (Lin, 2005) derived the exact frequency shift of an AFM non-uniform probe with an elastically restrained root, subjected to van der Waals force, and proposed the analytical method to determine the frequency shift of an AFM V-shaped probe scanning the relative inclined surface in non-contact mode (Lin, et al., 2006). Girard et al. (Girard, et al., 2006) studied dynamic atomic force microscopy operation based on high flexure modes vibration of the cantilever. Ilic et al. (Ilic, et al., 2007) explored the dynamic AFM cantilever interaction with high frequency nanomechanical systems and determined the vibration amplitude of the NEMS cantilever at resonance. Chang et al. (Chang & Chu, 2003) found an analytical solution of flexural vibration responses on tapped AFM cantilevers, and obtained the resonance frequency at arbitrary dimensions and tip radii. Wu et al. (Wu, et al., 2004) demonstrated a closed-form expression for the sensitivity of vibration modes using the relationship between the resonant frequency and contact stiffness of the cantilever and the sample. Horng (Horng, 2009) developed an analytical solution to deal with the flexural vibration problem of AFM cantilever during a nanomachining process by using the modal superposition method.

The above studies considered the AFM cantilever as a Bernoulli-Euler beam model. The effects of transverse shear deformation and rotary inertia were assumed to be negligible in

the analysis. However, for AFM-based cantilever direct mechanical nanomachining, the indentation and sampling of solid materials (e.g. polymer silicon and some metal surfaces) are performed. The effects of transverse shear deformation and rotary inertia in the vibration analysis should be taken into account for cantilevers whose cross-sectional dimensions are comparable to the lengths. Neglecting the effects of transverse shear deformation and rotary inertia in the vibration analysis may result in less accurate results. Hsu et al. (Hsu, et al., 2007) studied the modal frequencies of flexural vibration for an AFM cantilever using the Timoshenko beam theory and obtained a closed-form expression for the frequencies of vibration modes. However, the solution of the vibration response obtained using the modal superposition method for AFM cantilever modeled as a Timoshenko beam, and the response of flexural vibration of a rectangular AFM cantilever which has large shear deformation effects, are absent from the literature.

In this chapter, the response of flexural vibration of a rectangular AFM cantilever subjected to a sampling force is studied analytically by using the Timoshenko beam theory and the modal superposition method. Firstly, the governing equations of the Timoshenko beam model with coupled differential equations expressed in terms of the flexural displacement and the bending angle are uncoupled to produce the fourth order equation. Then, the sampling forces which are applied to the end region of the AFM cantilever by means of the tip, are transformed into an axial force, distributed transversal stress and bending stress. Finally, the response of the flexural vibration of a rectangular AFM cantilever subjected to a sampling force is solved using the modal superposition method. Moreover, a validity comparison for AFM cantilever modeling between the Timoshenko beam model and the Bernoulli-Euler beam model was conducted using the ratios of the Young's modulus to the shear modulus. From the results, the Bernoulli-Euler beam model is not suitable for AFM cantilever modeling, except when the ratios of the Young's modulus to the shear modulus are less than 1000. The Timoshenko beam model is a better choice for simulatimg the flexural vibration responses of AFM cantilever, especially for very small shear modulus.

## 2. Analysis

In contact mode, the AFM cantilever moves down by a small amplitude (1-5 nm) when the cantilever tip processes a sample surface. Therefore, the linear model can be used to describe the tip-sample interaction. The atomic force microscope cantilever, shown in Fig.1, is a small elastic beam with a length $L$, thickness $H$, width $b$, and a tip with a width of $w$ and length $h$. $x$ is the coordinate along the cantilever and $v(x,t)$ is the vertical deflection in the $x$-direction, as shown in Fig.2. One end of the cantilever, at $x = 0$, is clamped, while the other end, from $L - w$ to $L$, has a tip.

When the sampling is in progress, the tip makes contact with the specimen, resulting in a vertical reaction force, $F_y(t)$ and a horizontal reaction force, $F_x(t)$, both of which functions of time $t$. Assuming that the reaction forces act on the tip end, the product of the horizontal force and the tip length can form a bending stress on the bottom surface of the cantilever. The sampling system can be modeled as a flexural vibration motion of the cantilever. The motion is a function of mode shape and natural frequency, and its transverse displacement depends on time and the spatial coordinate $x$ [7 and 8]. When the sampling forces are

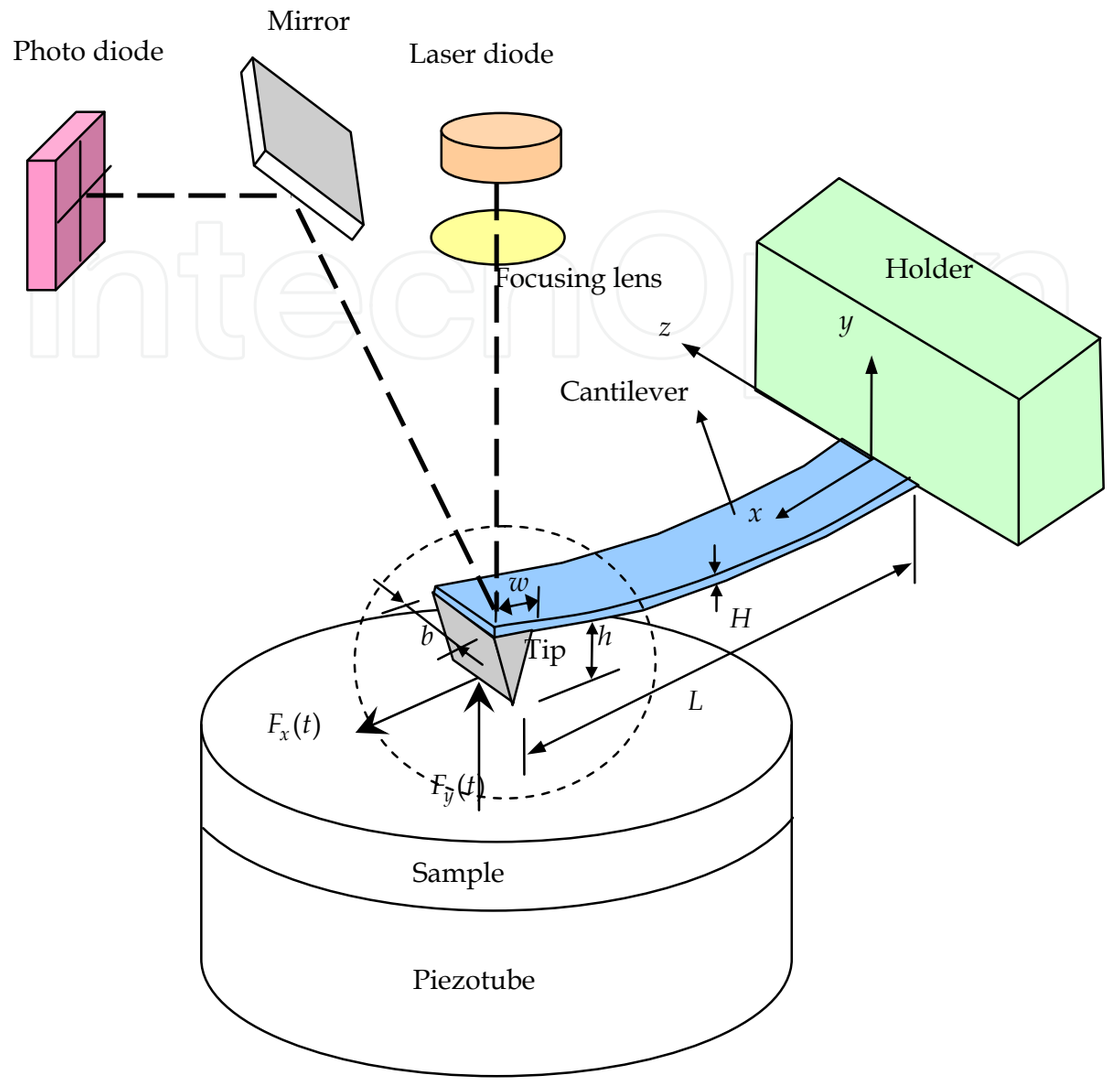


Fig. 1. Schematic diagram of an AFM tip-cantilever assembly processing a sample surface.

applied, the loads transmitted from the tip holder act on the end of the AFM cantilever, and can be modeled as the three parts shown in Fig.2, termed axial force $N(t)$, transverse excitation $p_l(x,t)$, and bending excitation $p_b(x,t)$.

Assuming that the transverse excitation is uniformly distributed on the bottom surface of the AFM cantilever, then it can be written as:

$$p_l(x,t) = F_y(t)u(x-L+w)/w, \tag{1}$$

where $u(x-L+w)$ is the unit step function.

The relationship between $F_x(t)$ and $F_y(t)$ can be expressed as $F_x = \frac{2\cos\theta}{\pi}F_y$ for a cone shape cantilever tip, where $\theta$ is the half-conic angle. The bending excitations, which result

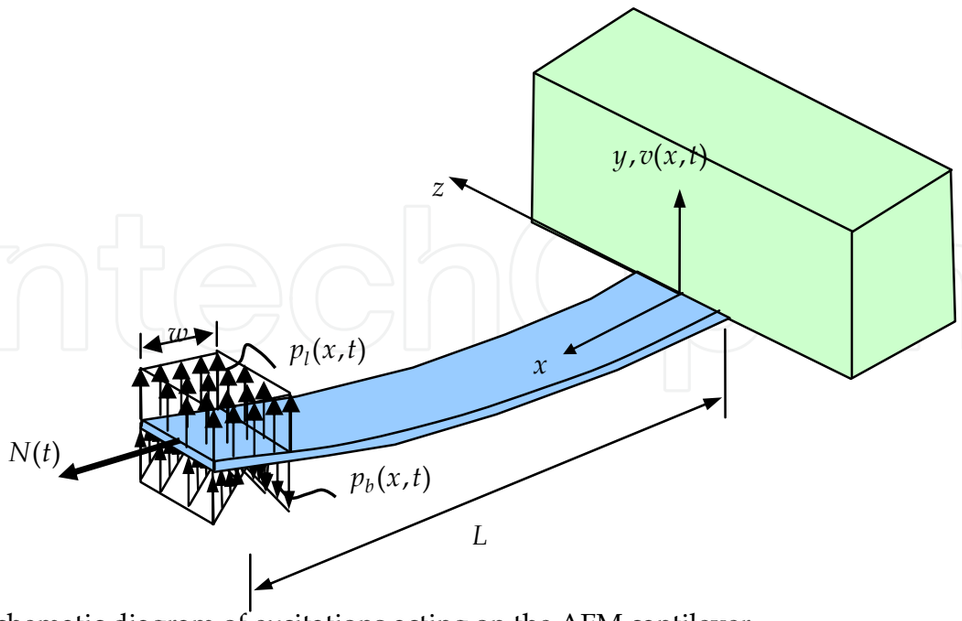


Fig. 2. Schematic diagram of excitations acting on the AFM cantilever

from the horizontal sampling force $F_x(t)$, act on the bottom surface of the AFM cantilever within the region from $L-w$ to $L$. They can be written as:

$$p_b(x,t) = \left[12h(2L-w-2x)\cos\theta / \pi w^3\right] F_y u(x-L+w) \tag{2}$$

By summing the above two excitations, the total transverse excitation $p_t(x,t)$ can be expressed as (Horng, 2009):

$$p_t(x,t) = C(x)F_y(t)u(x-L+w) \tag{3}$$

$$\text{where } C(x) = \frac{1+12h(2L-w)\cos\theta / \pi w^2}{w} - \frac{24h\cos\theta}{\pi w^3}x \tag{4}$$

Vibration behaviors of an AFM cantilever are examined using the Timoshenko beam theory. The effects of the rotary inertia and shear deformation are taken into account during contact with the sample. The governing equations of the Timoshenko beam model are two coupled differential equations expressed in terms of the flexural displacement and the angle of rotation due to bending. When the beam support is constrained to be fixed and all other external influences are set to zero, we obtain the classical coupled Timoshenko-beam partial differential equations (Hsu, et al., 2007):

$$\rho A\frac{\partial^2 v}{\partial t^2} - KAG\left(\frac{\partial^2 v}{\partial x^2} - \frac{\partial \psi}{\partial x}\right) = 0 \tag{5}$$

$$EI\frac{\partial^2 \psi}{\partial x^2} + KAG\left(\frac{\partial v}{\partial x} - \psi\right) - \rho I\frac{\partial^2 \psi}{\partial t^2} = 0 \tag{6}$$

where $x$ is the distance along the center of the cantilever, $v(x,t)$ is the transverse displacement, $t$ is time, $\psi(x,t)$ is the rotation of the neutral axis during bending, $E$ is Young's modulus, $G$ is shear modulus, $I$ is the area moment of inertia, $\rho$ is the volume density, $K$ is the shear factor ( $K$ = 5/6 for rectangular cross-section), and $A$ is the rectangular cross-sectional area of the cantilever.

Equations (5) and (6) may be uncoupled to produce a fourth order equation in $v(x,t)$. Considering the axial force effect, the classical uncoupled Timoshenko-beam partial differential equations can be written as (White, et al., 1995):

$$EI\frac{\partial^4 v(x,t)}{\partial x^4}+\rho A\frac{\partial^2 v(x,t)}{\partial t^2}-\frac{\partial}{\partial x}\left[N(t)\frac{\partial v(x,t)}{\partial x}\right]+$$

$$+\rho I\frac{\rho}{KG}\frac{\partial^4 v(x,t)}{\partial t^4}-\left(\rho I+\frac{\rho EI}{KG}\right)\frac{\partial^4 v(x,t)}{\partial x^2\partial t^2}=p_t(x,t) \tag{7}$$

where $N(t)=F_x(t)$ is the axial force.

The mode-superposition analysis of a distributed-parameter system is equivalent to that of a discrete-coordinate system once the mode shapes and frequencies have been determined because in both cases, the amplitudes of the modal-response components are used as generalized coordinates in defining the response of the structure. In principle, an infinite number of these coordinates are available for a distributed-parameter system, since it has an infinite number of modes of vibration. Practically, however, only those modal components which provide significant contributions to the response need be considered (Ray & Joseph, 1993 ; William, 1998). The essential operation of the mode-superposition analysis is the transformation from the geometric displacement coordinates to the modal-amplitude or normal coordinates. For a one-dimensional system, this transformation is expressed as:

$$v(x,t)=\sum_{n=1}^{\infty}\varphi_n(x)Y_n(t)=\sum_{n=1}^{\infty}q_n(x,t) \tag{8}$$

where $q_n(x,t)$ is the response contribution of the n-th mode, $Y_n(t)$ is the normal coordinate, and $\varphi_n(x)$ is the $n$-th mode shape of the AFM cantilever. In order to find the natural frequencies and mode shapes, the following non-dimensional variables are defined:

$$\xi=\frac{x}{L},\quad b^2=\frac{\rho AL^4}{EI}\omega^2,\quad r^2=\frac{I}{AL^2},\quad s^2=\frac{EI}{KAGL^2}. \tag{9}$$

Here $\xi$ is the non-dimensional length along the beam, and $\omega$ is the radian frequency. Then, $\varphi_n(x)$ can be given by (White, et al., 1995):

$$\varphi_n(\xi)=C\left[\cosh b_n\alpha\xi-\frac{(R_1-R_3)}{(R_2-RR_4)}\sinh b_n\alpha\xi-\cos b_n\beta\xi+\frac{R(R_1-R_3)}{(R_2-RR_4)}\sin b_n\beta\xi\right] \tag{10}$$

where $$\begin{Bmatrix}\alpha\\ \beta\end{Bmatrix} = (1/\sqrt{2})\left\{\mp(r^2+s^2)+[(r^2-s^2)^2+4/b_n{}^2]^{1/2}\right\}^{1/2} \tag{11}$$

$$R = \frac{(\alpha^2+s^2)}{\alpha}\frac{\beta}{(\beta^2-s^2)} \tag{12}$$

$$R_1 = (b_n/\alpha)\sinh b_n\alpha \tag{13}$$

$$R_2 = (b_n/\alpha)\cosh b_n\alpha \tag{14}$$

$$R_3 = (b_n/\beta)\sin b_n\beta \tag{15}$$

$$R_4 = -(b_n/\alpha)\cos b_n\beta \tag{16}$$

and $b_n$ are the non-dimensional natural frequencies, which can be obtained using the characteristic equation

$$\left(\frac{\alpha^2+s^2}{\alpha}\right)(R_3R_4' - R_3'R_4 + R_4R_1' - R_1R_4') + \left(\frac{\beta^2-s^2}{\beta}\right)(R_2R_3' - R_2'R_3 + R_1R_2' - R_2R_1') = 0 \tag{17}$$

where $$R_1' = [(\alpha^2+s^2)/\alpha]b_n\alpha\cosh b_n\alpha \tag{18}$$

$$R_2' = [(\alpha^2+s^2)/\alpha]b_n\alpha\sin b_n\alpha \tag{19}$$

$$R_3' = -[(\beta^2-s^2)/\beta]b_n\beta\cos b_n\beta \tag{20}$$

$$R_4' = -[(\beta^2-S^2)/\beta]b_n\beta\sin b_n\beta \tag{21}$$

Equation (8) simply states that any physically permissible displacement pattern can be modeled by superposing appropriate amplitudes of the vibration mode shapes for the structure. Substituting Eq. (8) into Eq. (7) and using orthogonally conditions gives

$$S_n\frac{d^4Y_n(t)}{dt^4} + (M_n+T_n)\frac{d^2Y_n(t)}{dt^2} + [-G_nF_x(t)+\omega_n^2M_n]Y_n(t) = P_n(t) \tag{22}$$

where $\omega_n$ is the $n$-th mode natural frequency of the AFM cantilever obtained using:

$$\omega_n = b_n\sqrt{\frac{EI}{\rho AL^4}} \tag{23}$$

$S_n$, $M_n$, $T_n$ and $p_n$ are the generalized constants of the $n$-th mode, given by

$$S_n = (\rho I\frac{\rho}{KG})\int_0^L \varphi_n(x)^2\,dx \tag{24}$$

$$M_n = (\rho A)\int_0^L \varphi_n(x)^2\,dx \tag{25}$$

$$T_n = (\rho I + \frac{\rho EI}{KG})\int_0^L \varphi_n(x)\frac{d^2\varphi_n(x)}{dx^2}\,dx \tag{26}$$

$$G_n(t) = \int_0^L \left[\varphi_n(x)\frac{d^2\varphi_n(x)}{dx^2}\right]dx \tag{27}$$

$$P_n(t) = \int_0^L \varphi_n(x)p_t(x,t)dx \tag{28}$$

Using Eq. (3) and Eq. (4), Eq. (28) can be rewritten as

$$P_n(t) = c_n F_y(t) \tag{29}$$

where

$$c_n = \int_0^L \varphi_n(x)\left(\frac{1+12h(2L-w)\cos\theta/\pi w^2}{w} - \frac{24h\cos\theta}{\pi w^3}x\right)u(x-L+w)dx \tag{30}$$

Then, the Normal-Coordinate Response Equation, which is exactly the same equation considered for the discrete-parameter case, can be solved.

$$\frac{d^4Y_n(t)}{dt^4} + (M_n + T_n)/S_n\frac{d^2Y_n(t)}{dt^2} + \frac{[-G_nF_x(t) + \omega_n^2 M_n]}{S_n}Y_n(t) = c_nF_y(t)/S_n \tag{31}$$

Assuming a zero initial condition, with $v(x,0)=0$, $\dot{v}(x,0)=0$, $\ddot{v}(x,0)=0$ and $\dddot{v}(x,0)=0$, and providing that the sampling force $F_y(t)$ is a series of harmonics, $F_y(t)$ can be written as:

$$F_y(t) = \sum_{i=1}^{m} F_i \sin(\omega_i t) \tag{32}$$

When the *j-th* excitation frequency $\omega_j$ is equal to the n-th natural frequency $\omega_n$, the Runge-Kutta method is introduced to solve the above fourth-order system.

## 3. Results and discussion

The main goal of this study is to analyze the flexural vibration responses in nanoscale processing using atomic force microscopy modeled as a Timoshenko beam. To demonstrate the validity of the analytical solution, numerical computations were performed. The geometric and material parameters considered were as follows:

$E = 170Gpa$, $\bar{m} = 0.2898km/\mu m$, $\rho = 2300km/m^3$, $L = 125\mu m$, $b = 30\mu m$, $H = 4.2\mu m$, $h = 5\mu m$, $2\theta = 30^\circ$ and $m = 3$, $F_i = 1000/(2i-1)\times 10^{-9}$.

The modulus-ratio $REG$, defined as the ratio of $E$ to $G$ (i.e. $REG = E/G$), is introduced to define the values of shear modulus $G$ and to describe the effects of shear deformation. In this

study, the flexural vibration responses at the end of the AFM cantilever were obtained using the contribution of the first five vibration modes. A non-dimensional response was used to normalize the static response as given in $F_1 L^3 / (3EI)$, and $\omega_i = (2i-1) \times r\omega_n$, and set as the simulated values of the excitation frequency of the vertical sampling force. Thus, $F_y(t)$ is taken as:

$$F_y(t) = 1000\left( \sin r\omega_n t + \frac{1}{3}\sin 3 \times r\omega_n t + \frac{1}{5}\sin 5 \times r\omega_n t \right)(nN) \tag{33}$$

where *r* is the frequency ratio that can used to describe the deviation between the excitation frequency and modal frequencies. The modal frequency $\omega_n$ and modal shapes $\varphi(x)$ of the first five vibration modes for an AFM cantilever are shown in Fig.3 and Fig.4, respectively.

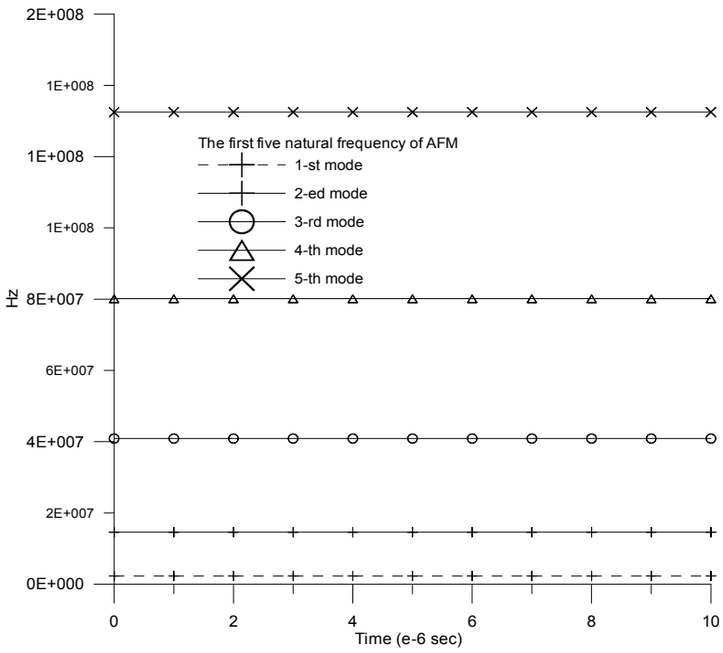


Fig. 3. Natural frequencies of the first five vibration modes for an AFM cantilever.

In order to investigate the effects of transverse shear deformation, the response histories at the end point of the AFM cantilever between different small and large modulus-ratios, with respect to excitation frequencies far away from( $r = 0.1$) and close to ( $r = 0.9$) the first natural frequency, are shown in Fig.5 to Fig.8. Figure 5 and Fig.6 indicate that the responses are similar for the various modulus-ratios when they are less than 1000. This means that if the effects of transverse shear deformation are small enough to be negligible, the Timoshenko beam model can be reduced to the Bernoulli-Euler beam model. Figure 6 also reveals that the resonance effect occurs when the AFM cantilever has small modulus-ratios and the excitation frequencies are close to the modal frequencies.

Figure 7 and Fig.8 show the response histories at the end point of the AFM cantilever between different large modulus-ratios for excitation frequencies far away from ( $r = 0.1$) and close to ( $r = 0.9$) the first modal frequency, respectively. The results are quite different

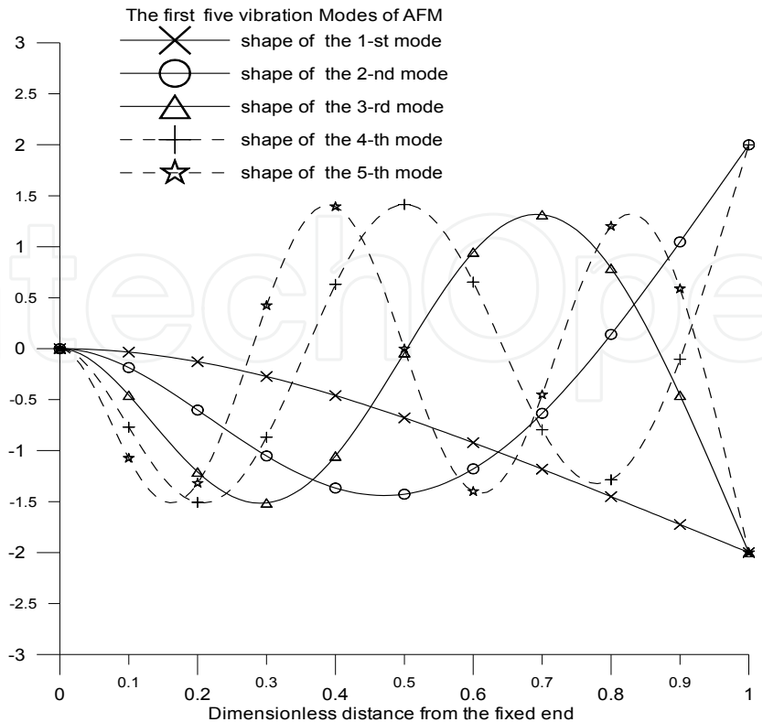


Fig. 4. The shape of the first five vibration modes for an AFM cantilever.

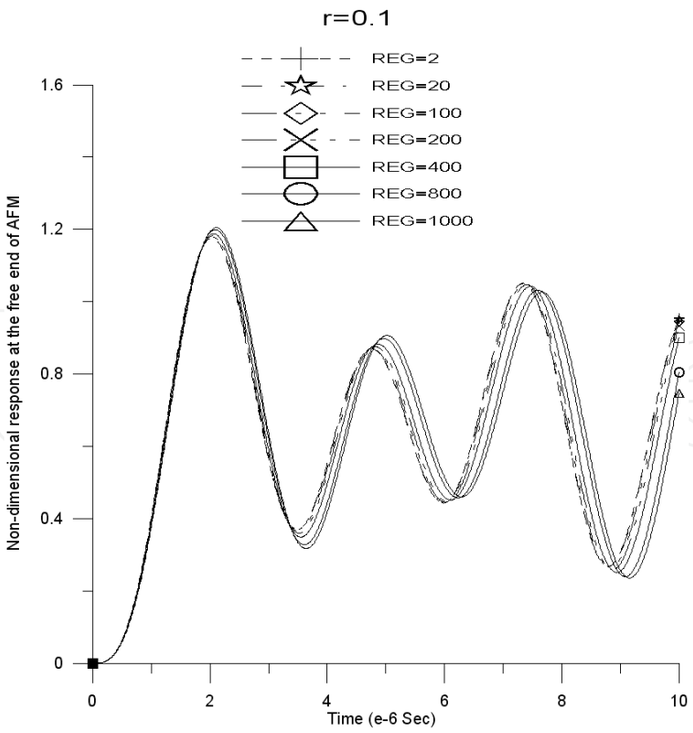


Fig. 5. The effect of various small modulus-ratios ( $REG$ ) on the response of the end point for the excitation frequency far away from the first natural frequency, i.e. $0.1\omega_1$ .

from those of Fig.5 and Fig.6. Figure 7 indicates that the magnitude of the transversal response increases and its oscillating frequency decreases when the modulus-ratio increases. This is because that large shear deformation increases the transversal response, which slows down the oscillating frequency when the excitation frequency is far away from the natural frequency. However, Fig. 8 tells us that the magnitude of the transversal response decreases and its oscillating frequency becomes small when the modulus-ratio increases. The reason for this is that the effects of resonance were counteracted by the transverse shear deformation, resulting in the small transversal response when the AFM cantilever has the sufficiently large modulus-ratios and the excitation frequencies of AFM cantilever are close to the modal frequencies. Consequently, Fig.7 and Fig.8 imply that when a sufficiently small shear modulus is used in AFM cantilever, the effect of transverse shear deformation has a significant effect on the transversal response and the Timoshenko beam model is the proper choice for simulating AFM cantilever dynamic behavior.

Figures 9 shows the effects of various tip holder widths, $w$ , on the response of the end point. The widths are normalized by the length of the AFM cantilever. Fig.9 shows that the response at the free end decreases as the width of the tip increases. Therefore, an AFM cantilever with a large tip width is suggested to reduce the response at the end of the AFM cantilever. Figure 10 shows the response histories at the end point of the AFM tip for various tip lengths $h$ . From the simulation results shown in Fig.10, the responses are relatively small when the tip length is large. This is due to a large tip length producing large bending effects. Therefore, an AFM tip with large tip length is suggested to reduce the response at the end of the AFM cantilever.

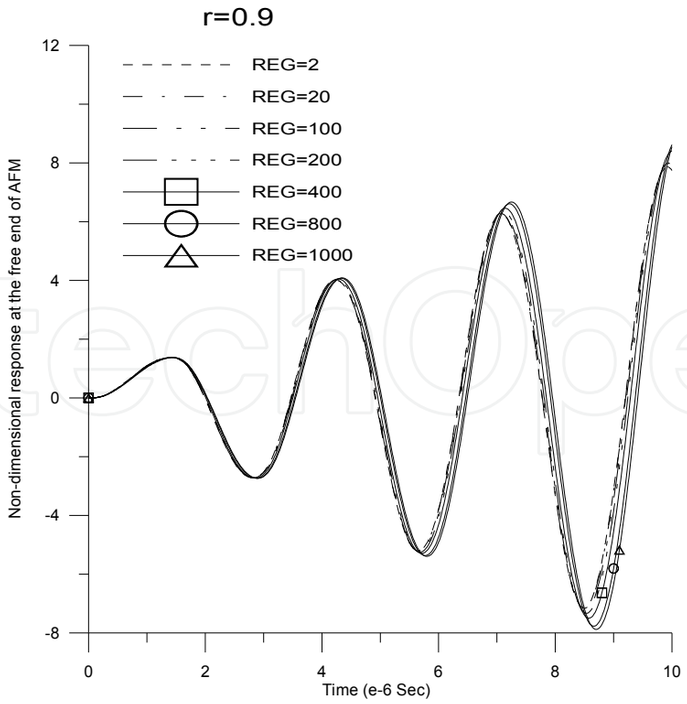


Fig. 6. The effect of various small modulus-ratios ( $REG$ ) on the response of the end point for the excitation frequency close to the first natural frequency, i.e. $0.9\omega_1$ .

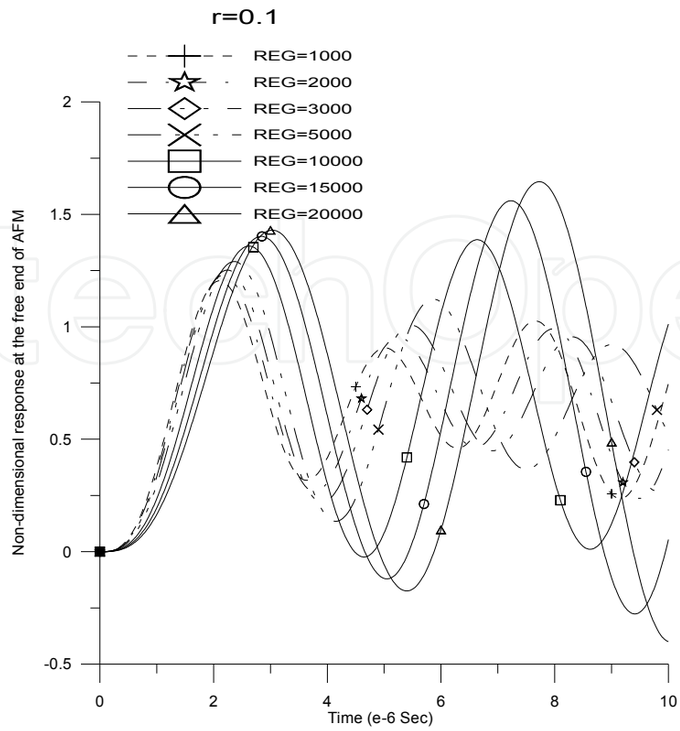


Fig. 7. The effect of various large modulus-ratio ( $REG$ ) on the response of the end point for the excitation frequency far away from the first natural frequency, i.e. $0.1\omega_1$

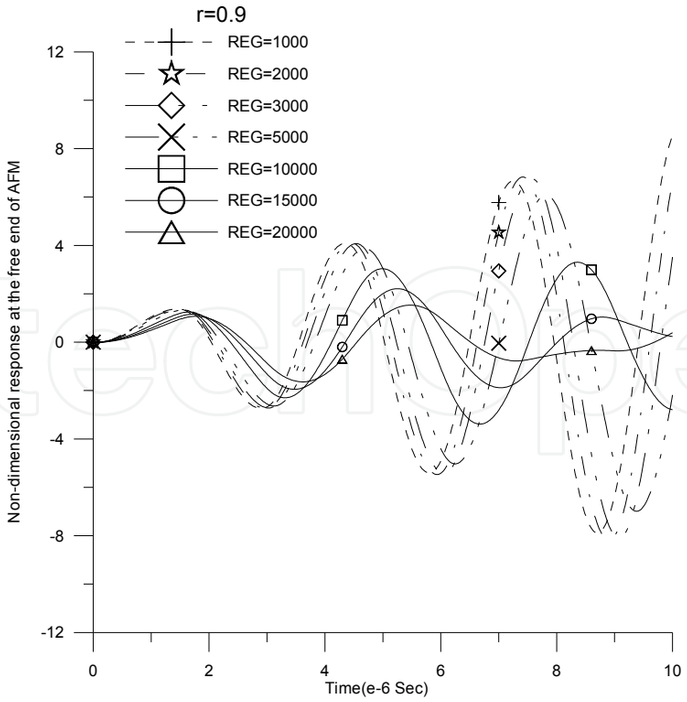


Fig. 8. The effect of various large modulus-ratio ( $REG$ ) on the response of the end point for the excitation frequency which is close to the first natural frequency, i.e. $0.9\omega_1$ .

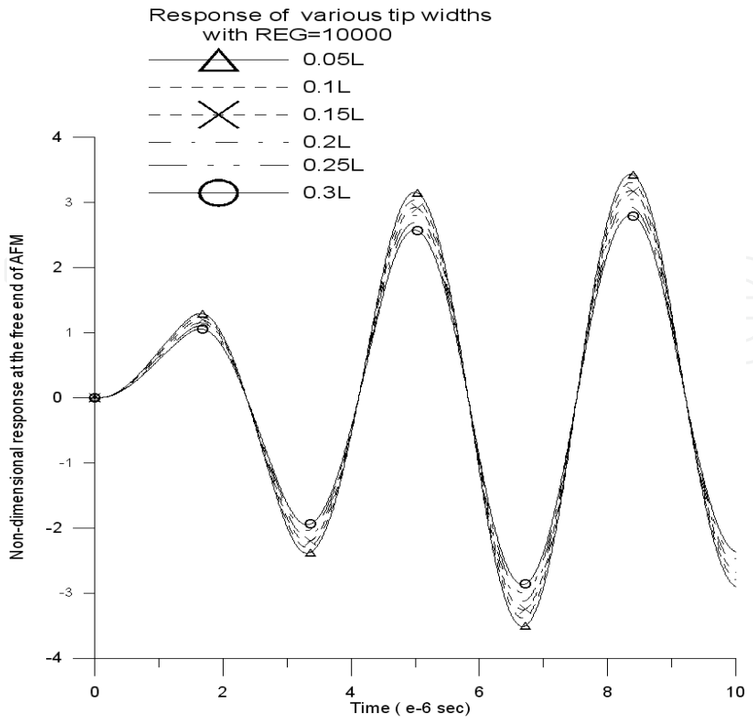


Fig. 9. Response histories at the end point for various tip widths with $REG = 10000$ .

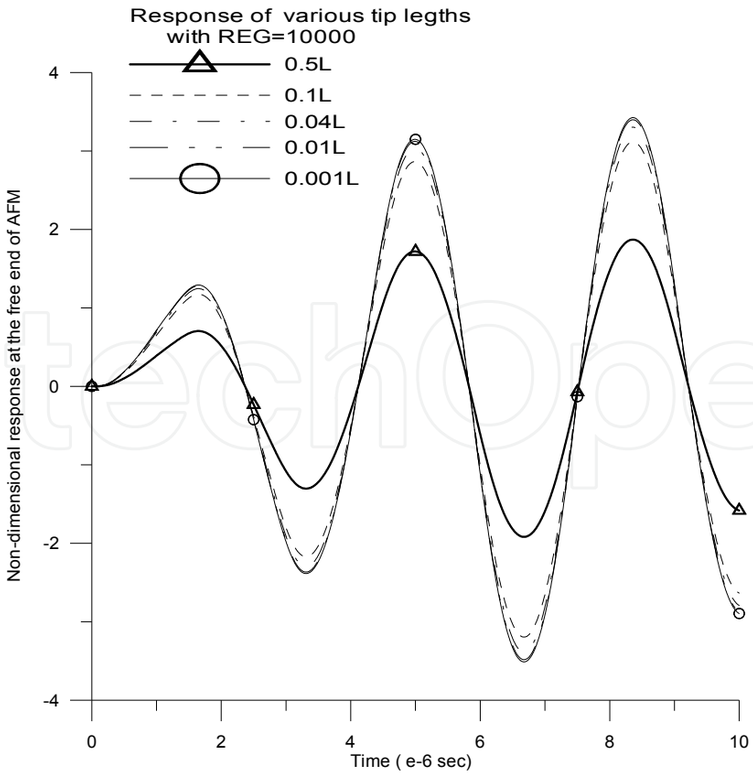


Fig. 10. Response histories at the end point for various tip lengths with $REG = 10000$ .

## 4. Conclusions

The modal superposition method and the Timoshenko beam theory were applied to determine the flexural vibration responses at the end of the AFM cantilever during AFM-based nanoprocessing process. As expected, the Bernoulli-Euler beam model for AFM cantilever applies to the small effects of transverse shear deformation, but not for modulus-ratios greater than 1000. When modulus-ratios are greater than 1000, the Timoshenko beam model is the proper choice for simulating the flexural vibration responses of AFM cantilever. Moreover, the oscillating frequency of transversal response decreases due to the transverse shear deformation and the magnitudes of the transversal response depend on the deviation between the excitation frequencies and the modal frequencies. In conclusion, one can reduce the response at the end of AFM cantilever by decreasing the shear modulus when the frequencies of processing are far away from the modal frequencies, and by increasing the shear modulus when the frequencies of processing are close to the modal frequencies. Furthermore, an AFM cantilever with a large tip width and length is suitable for reducing the response at the end of the AFM cantilever.

## 5. Acknowledgements

This work was supported by the National Science Council, Taiwan, Republic of China, under grant NSC 99-2221-E-168-021.

## 6. References

Chang, W.J. & Chu, S.S. (2003). Analytical solution of flexural vibration response on taped atomic force microscope cantilevers, Phys. Letter A. Vol. 309, pp. 133-137.

Fang, T.H. & Chang, W.J. (2003). Effects of AFM-based nanomachining process on aluminum surface, J. Phys. Chem. Solids, *J. Phys. Chem. Solids*, Vol. 64 913-918.

Girard, P.; Ramonda, M. & R. Arinero, (2006). Dynamic atomic force microscopy operation based on high flexure modes of the cantilever, *Rev. Sci. Instrum.* Vol. 77, 096105.

Horng, T.L. (2009). Analytical Solution of Flexural Vibration Responses on Nanoscale Processing Using Atomic Force Microscopy, *J. Mater. Pro. Tech.*, Vol. 209, pp. 2940-2945.

Horng, T.L. (2009). Analyses of Vibration Responses on Nanoscale Processing in a Liquid Using Tapping-Mode Atomic Force Microscopy, *Appl. Surf. Sci.* Vol. 256 311-317.

Hsu, J.C.; Lee, H.L.& Chang, W.J. (2007). Flexural Vibration Frequency of Atomic Force Microscope Cantilevers Using the Timoshenko Beam Model, *Nanotechnology.* Vol. 18, 285503.

Ilic, B.; Krylov, S.; Bellan L.M. & H.G. Craighead, (2007). Dynamic characterization of nanoelectromechanical oscillators by atomic force microscopy, J. *Appl. Phys.* Vol. 101, 044308

Kageshima, M.; Jensenius, H.; Dienwiebel, M.; Nakayama, Y.; Tokumoto, H. ; Jarvis, S.P. & Oosterkamp, T.H. (2002). Noncontact atomic force microscopy in liquid environment with quartz tuning fork and carbon nanotube probe. *Appl. Surf. Sci.* Vol. 188, pp.440-444.

Kobayashi, K.; Yamada, H. & Matsushige, K. (2002). Dynamic force microscopy using FM detection in various environments. Appl. Surf. Sci. Vol.188, pp. 430-434.

Lin, S.M. (2005). Exact Solution of the frequency shift in dynamic force microscopy, *Appl. Surf. Sci.* Vol. 250, pp. 228-237.

Lin, S.M.; Lee. S.Y. & B-S Chen, (2006). Closed-form solutions for the frequency shift of V-shaped probes scanning an inclined surface, *Appl. Surf. Sci*. Vol. 252 6249-6259.

Miyahara, K.; Nagashima, N.; Ohmura T. & Matsuoka, S. (1999). Evaluation of mechanical properties in nanometer scale using AFM-based nanoindentation tester, *Nanostruct. Mater.* Vol. 12, pp.1049-1052.

Ray, W. & Joseph, P. (1993). Dynamic of Structure, second ed., McGraw-Hill, Inc., New Jersey.

Takaharu Okajima; Hiroshi Sekiguchi; Hideo Arakawa & Atsushi Ikai. (2003). Self-oscillation technique for AFM in liquids. *Appl. Surf. Sci.* Vol. 210, pp.68-72.

White, M. W. D. & Heppler, G. R. (1995). Vibration Modes and Frequencies of Timoshenko Beams with Attached Rigid Bodies, *ASME J. Appl. Mech.* Vol. 62, pp.193-199.

William, T. (1998). Theory of Vibrations with Application, fifth ed., Prentice Hall, New Jersey.

Wu, T.S.; Chang, W.J. & J.C. Hsu, (2004). Effect of tip length and normal and lateral contact stiffness on the flexural vibration response of atomic force microscope cantilevers, *Microelectronic Eng.* Vol. 71, pp.15-20.

Yaxin Song & Bharat Bhushan, (2007). Finite-element vibration analysis of tapping-mode atomic force microscopy in liquid, *Ultramicroscopy.* Vol. 107, pp. 1095-1104.

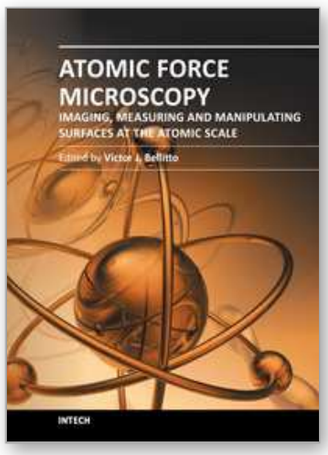


**Atomic Force Microscopy - Imaging, Measuring and Manipulating Surfaces at the Atomic Scale**

Edited by Dr. Victor Bellitto

ISBN 978-953-51-0414-8
Hard cover, 256 pages
**Publisher** InTech
**Published online** 23, March, 2012
**Published in print edition** March, 2012

With the advent of the atomic force microscope (AFM) came an extremely valuable analytical resource and technique useful for the qualitative and quantitative surface analysis with sub-nanometer resolution. In addition, samples studied with an AFM do not require any special pretreatments that may alter or damage the sample and permits a three dimensional investigation of the surface. This book presents a collection of current research from scientists throughout the world that employ atomic force microscopy in their investigations. The technique has become widely accepted and used in obtaining valuable data in a wide variety of fields. It is impressive to see how, in a short time period since its development in 1986, it has proliferated and found many uses throughout manufacturing, research and development.



**InTech Europe**
University Campus STeP Ri
Slavka Krautzeka 83/A
51000 Rijeka, Croatia
Phone: +385 (51) 770 447
Fax: +385 (51) 686 166
www.intechopen.com

**InTech China**
Unit 405, Office Block, Hotel Equatorial Shanghai
No.65, Yan An Road (West), Shanghai, 200040, China
中国上海市延安西路65号上海国际贵都大饭店办公楼405单元
Phone: +86-21-62489820
Fax: +86-21-62489821

IntechOpen